A. Significance

In the November 2015, Naho Tamura penned an article entitled "*What's it like to be absent? - A message from an "ex"-patient*"[3]. We learn from her about the destructive impact that childhood absence epilepsy, a disorder that affects 1 in every 1,000 children[28], has on a young child's life. She recounts 13 years during which valproic acid controlled her seizures, but also produced so many side effects (deep drowsiness, inattention, forgetfulness) that she questions whether her childhood would have been better without drug intervention.

And yet, Naho Tamura's story is considered one of success. In aggregate, the most common anti-seizure drugs fail to treat the majority of patients with childhood absence epilepsy[1]. Either medication is reasonably effective but has intolerable side effects (e.g. valproic acid), or is better tolerated but not very effective (e.g. lamotrigine). Clearly, better therapies are required.

Rodent work highlights the critical need to consider that diet – low blood glucose in particular – may be an "environmental risk factor" that precipitates absence seizures[13]. Indeed, it has been argued that blood glucose stabilization may be an effective adjunct therapy to treat absence epilepsy[13]. Considering the poor effectiveness of anti-seizure drugs in treating the disorder, such a strategy is worthy of careful examination.

Clinical reports also link glucose dysregulation to absence seizures. In 1991, De Vivo et al. first characterized patients with glucose transporter 1 deficiency syndrome (Glut1-DS)[29], a disorder characterized by the functional loss of glucose transporter 1 (Glut-1), the carrier primarily responsible for shuttling glucose across the blood-brain barrier[30,31]. Electroencephalogram (EEG) recordings from these patients reveal frequent 2-4 Hz spike-and-wave discharges (SWDs)[29,32,33], the principal feature of absence seizures[34-36]. More recent studies have revealed that one in 10 patients with early onset absence epilepsy has Glut1 deficiency[37,38].

The thalamus, a subcortical brain structure, is particularly sensitive to hypoglycemia. First, Pascual et al. used cerebral [^{18}F]-fluorodeoxyglucose positron emission tomography (PET) to show that the thalamus, along with certain cortical regions, is particularly hypometabolic in patients with Glut1-DS[33]. Indeed, the authors argue that dysregulated glucose metabolism associated with thalamocortical circuits is quite likely the primary driver of Glut1-DS-associated absence seizures. Second, hypoglycemia-associated thalamic activation also occurs in non-pathological conditions. [^{15}O]water-PET studies reveal that even slightly hypoglycemic conditions in healthy patients selectively elevates putative synaptic activity in the thalamus[16-18].

In aggregate, the aforementioned studies strongly implicate a role for glucose regulation of both (1) absence seizures, and (2) thalamocortical brain circuits. Indeed, they strengthen the long-appreciated, intimate association between the two[19,24,25,34,39-43]. Thus, if thalamocortical circuits are highly glucose sensitive, then it is the *expectation* that absence seizures would in turn be sensitive to levels of glucose.

What remains surprising, however, is that to date *no cellular studies targeted at understanding how glucose regulates neural excitability in the thalamus have been carried out*. And yet, the aforementioned work reveals a strong link between glucose handling in the thalamus and absence seizures. We aim to interrogate this link, with the goal of identifying the mechanisms by which energy metabolism regulates absence seizures. Our work addresses several fundamental questions, including:

(1) Are absence seizures specifically sensitive to glucose levels or, instead, are they sensitive to other energy substrates mobilized when blood glucose drops (e.g. ketone bodies)?

(2) How are thalamocortical circuits recruited at the cellular level during hypoglycemia?

(3) Does the effectiveness of anti-seizure drugs change during hypoglycemia?

We believe our laboratory has the appropriate tools and expertise to successfully address these questions.

B. Innovation

We aim to determine how energy metabolism regulates a critical seizure-generating node associated with childhood absence epilepsy. We consider this goal innovative because to our knowledge we are the first group to tackle this objective using the electrophysiological and imaging tools necessary to dissect neural circuit excitability at the cellular level. Moreover, successful completion of the proposed research will facilitate the development of a new conceptual understanding of a disorder whose mechanisms have largely evaded researchers since the first EEG recordings of spike-and-wave seizures more than eighty years ago[36].

We will use a comprehensive approach to evaluate how energy metabolism regulates thalamocortical seizures. First, we are using modern standards for seizure evaluation in rodents (i.e. video-EEG) in a dedicated facility that we have designed. Therein, we perform both conventional, tethered EEG experiments as well as state-of-the-art wireless EEG telemetry, the latter of which we have recently published using[44]. While we still evaluate our seizure data manually, we continue to develop Linux- and Matlab-based algorithms to facilitate this process. We manage all video-EEG data with several dedicated, multi-core Linux servers with

>50 terabytes of disk space. Thus, while video-EEG is arguably not itself innovative, our lab performs such experiments at the leading-edge of what is considered rigorous rodent seizure work.

Likewise, with regard to our *in vitro* electrophysiological approaches, we execute patch clamp recordings, the gold standard for assessing neuronal excitability at the cellular level. We routinely perform patch clamp recordings, both in the conventional, whole-cell configuration, as well as in the cell-attached and perforated-patch configurations. We have developed several Matlab-based algorithms that interface with pClamp software to permit online measurement of cellular properties (i.e. action and synaptic potentials). We make these tools freely available at *www.beenhakkerlab.pharm.virginia.edu*.

The primary technological innovation we present stems from our capacity to utilize calcium-imaging techniques to query neural circuits in the thalamus. Using viral approaches, we can take advantage of both mouse and rat models of epilepsy. We express GCaMP6f, the current iteration of genetically-encoded calcium indicators, in the thalamus of rodents as young as ten days old (**Fig. 11**). To achieve this early expression, we introduce the vector within one day of birth using the intracerebroventricular injection approach[45].

We utilize both *in vitro* and *in vivo* imaging techniques to examine circuit excitability. First, we rapidly image large populations of thalamic neurons within brain slices with an sCMOS camera (100 frames per second, full-frame). Image analyses are performed on dedicated servers with custom tools we make available online. For *in vivo* optical recordings of thalamic activity, we utilize recently-developed fiber photometry techniques to image GCaMP signals[46]. Notably, we have recently developed approaches to couple subcortical fiber photometry with EEG to simultaneously image thalamic circuits and record absence seizures (**Fig. 11**).

In sum, we believe we have amassed a comprehensive set of state-of-the-art tools, both practical as well as quantitative, to systematically identify mechanisms by which energy metabolism regulates absence seizures.

C. Approach

1. Conceptual Framework

We approach our project with the hypothesis that the epileptic brain experiences episodic states during which the probability of seizure genesis is elevated. In agreement with our hypothesis, some argue that epilepsy researchers "*need to expand the experimentally-derived idea of time-invariant [neuronal] imbalances*" to also understand how the timing of seizures is governed by episodic shifts in the balance of neuronal activity[26]. Continuously-fluctuating energy substrates are likely candidates to establish ictogenic states in the metabolically-demanding brain.

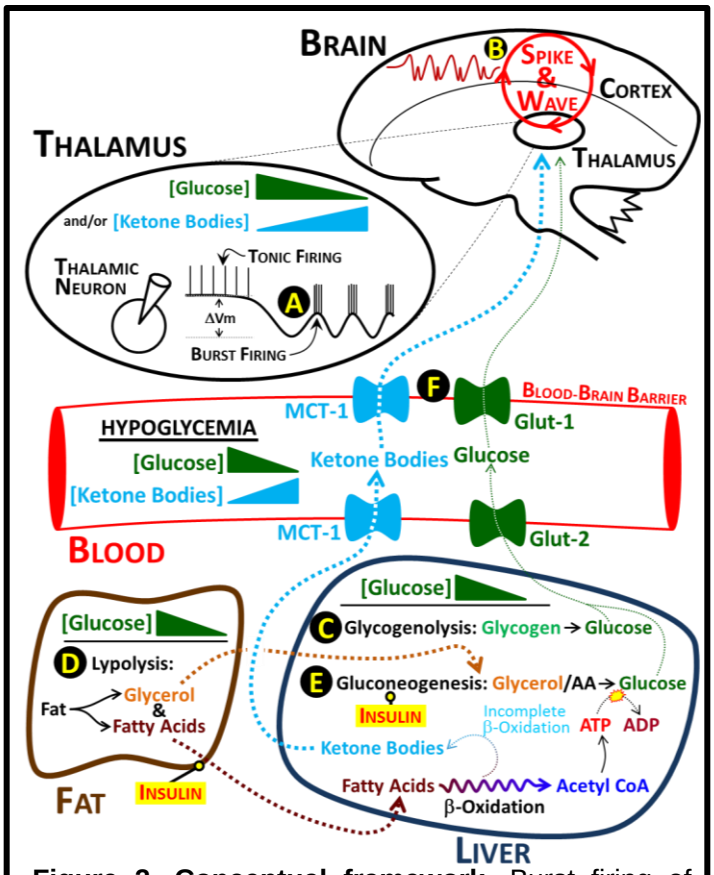

Figure 2. Conceptual framework. Burst firing of thalamic neurons **(A)** is associated with absence seizure-related SWDs **(B)**. Studies show low blood glucose increases activity in the thalamus. During hypoglycemia, the liver undergoes *glycogenolysis* **(C)** to produce glucose from stored glycogen. Additionally, fat is broken down into glycerol and fatty acids during lipolysis **(D)**. Fatty acids then undergo β-oxidation in the liver to produce ATP used to drive *gluconeogenesis* **(E)**, the process by which amino acids (AA) and glycerol are converted into glucose. If β-oxidation of fatty acids is incomplete, then ketone bodies are generated. Glucose and ketone bodies are transported across the blood-brain barrier **(F)** by Glut-1 and MCT-1, respectively. Insulin blocks both gluconeogenesis and fatty acid transport from fat.

Glucose is the preferred fuel of the brain. Glucose transported into the brain is mainly provided by diet and, during fasting, by the liver (**Fig. 2**). During hypoglycemia, liver glycogen is broken down (i.e. *glycogenolysis*) and serves to maintain normal blood glucose levels. As glycogen is depleted, *gluconeogenesis* is initiated[47,48]. This latter process primarily takes place in the liver, producing glucose from amino acids and glycerol. To support gluconeogenesis, the liver increases β-oxidation of fatty acids to yield ATP. *Incomplete* β-oxidation yields three water-soluble ketone bodies: acetoacetate, β-hydroxybutyrate (βHB) and acetone. These three molecules are effective energy substrates that provide an alternative fuel source that can accommodate nearly half of the brain's energy requirements[49]. Thus, during hypoglycemia, the brain experiences low glucose concentrations and high ketone body concentrations[49].

Neuronal activity can be altered by glucose[50-53] and ketone bodies[54-58]; thus either energy substrate could alter the excitability of thalamocortical circuits (**Fig. 2**). The thalamus contains many discrete nuclei that are devoted to sensory processing[41]. Additionally, the thalamus is intimately associated with spike-and-wave discharges (SWDs) commonly observed in childhood and juvenile absence epilepsy.

Thalamic circuits are critically involved in the generation of SWDs[19,20,25,41]. Reticular thalamic (RT) neurons and thalamocortical (TC) neurons of the dorsal thalamic nuclei exhibit two modes of action potential-mediated (*spiking*) activity known as tonic- and burst-firing. The mode is often dictated by the neuron's resting membrane potential (**Fig. 2**), which in turn is defined by the local modulatory state of the thalamus[59,60]. Tonic mode, characterized by a depolarized resting membrane potential and regular spiking, is associated with the awake state. Burst mode, marked by a hyperpolarized resting membrane potential and brief, high-frequency barrages of action potentials, is associated with spike-and-wave seizures.

Figure 2 demonstrates how multiple mechanisms can account for seizure modulation during hypoglycemia. One fundamental question is whether thalamocortical circuits are tuned to levels of glucose, ketone bodies, or both. *Our data support the hypothesis that absence seizures are triggered specifically by low blood glucose.*

2. Preliminary Data

2.1. Data supporting Aim 1 (Hypothesis: *Low blood sugar is the primary trigger for elevated absence seizures during acute fasting*).

We begin with two goals: **(1)** determine the robustness of the observation that acute fasting increases the SWD occurrence in animals predisposed to have seizures; and **(2)** define parameters that contribute to fasting-induced seizures. To address the first goal, we performed parallel experiments in two genetic models of absence seizures. The first model is the seizure prone DBA/2J mouse[13,61,62]. The second is the well-characterized WAG/Rij rat[63-66]. If fasting triggers seizures across species, then this finding bolsters the relevance of our study to human patients.

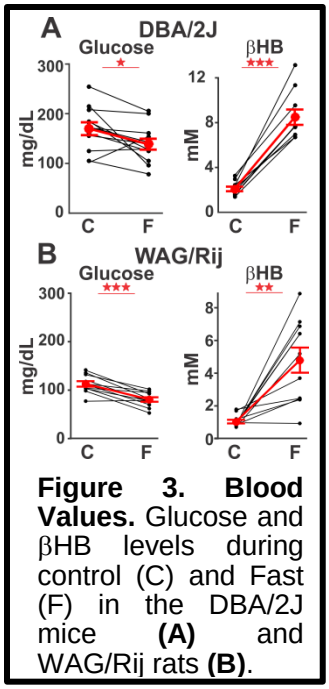

Figure 3. Blood Values. Glucose and βHB levels during control (C) and Fast (F) in the DBA/2J mice **(A)** and WAG/Rij rats **(B)**.

2.1.A. Fasting induces hypoglycemia & ketoacidosis in both animal models.

Blood measurements agreed with the well-described response to an acute fast[47] (**Fig. 3**). Consistent with previous reports in DBA/2J mice[13], glucose dropped by 18% following the 16-hour fast (p=0.029, n=12). Concomitant with lower blood glucose was a pronounced increase in blood ketone bodies (p<0.001, n=12, **Fig. 3**). βHB was used as a measure of overall ketoacidosis[67].

Fasting WAG/Rij rats had a similar impact on blood measurements. Glucose levels dropped 31% in response to a 22 hour fast (p=0.001, n=11, **Fig. 3**); ketone bodies increased by 5.4±1.0 fold (mean±S.E.M, p=0.001, n=11, **Fig. 3**). Thus, in two absence seizure rodent models, acute food withdrawal produces hypoglycemia and ketoacidosis. The latter may modulate some seizure disorders[23].

2.1.B. Fasting exacerbates seizures in multiple animal models.

We measured SWDs before and during the fast in a subset of the aforementioned animals. Seizures were monitored using video-EEG during a 5-hour epoch throughout the fed and fasted periods (**Fig. 4A**). EEGs were scored by multiple blinded observers for the occurrence of SWDs (**Fig. 4B**). SWDs matched electrographic events previously described[13,61-66]; events were associated with behavioral arrest.

Both seizure models produced more SWDs during the fast (**Fig. 4C&D**). Fasting increased the number of events by 3.3±0.6 fold in DBA/2J mice (mean±S.E.M, n=10, **Fig. 4D**), and by 2.6±1.1 fold in WAG/Rij rats (n=6, **Fig. 4D**). Events became prolonged in mice, but not in rats (**Fig. 4D**). Seizure burden, the total seizure duration during the recording period, increased by 4.1±1.02 fold and 3.5±1.1 fold in the DBA/2J and WAG/Rij models, respectively. Thus, fasting promotes SWDs across species, increasing potential relevance to the human condition. Additionally, these findings allow proposed mechanistic experiments (see Specific Aims) in the larger, experimentally-tractable rat.

2.1.C. Hypoglycemia, not ketoacidosis, exacerbates seizures.

At first glance, the concomitant changes in blood glucose and ketone bodies present a challenge to defining SWD-exacerbating mechanism(s). Indeed, a plot of the fasting-induced change in either glucose or βHB (%Δ Glucose or %Δ βHB) versus the change in seizure count (%Δ # Seizures) reveals in both species an association with elevated seizures (decrease in glucose, increase in βHB, **Fig. 5A&B**). If both associations exist, then is it possible to determine whether *either* glucose *or* βHB levels drive the observed seizure change?

In an attempt to dissociate seizures from ketoacidosis, we correlated the two parameters in fed WAG/Rij rats injected with insulin. Insulin, by promoting glycogen synthesis in the liver and glucose uptake into muscle and fat, decreases blood glucose levels. Insulin also inhibits gluconeogenesis and lipolysis (see **Fig. 2**). From these

collective actions, we hypothesized that insulin would decrease blood glucose *without* concomitantly increasing ketone bodies.

The schematic in **Figure 6A** details our experimental protocol. We collected blood for glucose/βHB measurements and recorded video-EEGs shortly thereafter. After one hour of recording, we injected WAG/Rij rats with saline (day 1) and insulin (day 2). We collected blood once again 90 minutes following the injection (i.e. 2.5 hours into the recording).

Animals injected with insulin produced more SWDs than those injected with saline (**Fig. 6B&C**). Indeed, we observed an increase in discharge count shortly after the insulin injection (compare seizure raster before and after insulin injection, **Fig. 6B**, **right**). Quantification showed that SWD count increased 2.6±0.4 fold following insulin injection relative to saline injection (p=0.043, **Fig. 6C**). As in the fasted experiment, SWD duration did not change.

Importantly, saline injection into WAG/Rij rats did not change glucose or βHB levels, whereas insulin changed only blood glucose; βHB levels remained the same following insulin. These findings indicate that lower blood glucose, and not higher ketone bodies, exacerbates seizures. Compare **Figures 5B & 5C**.

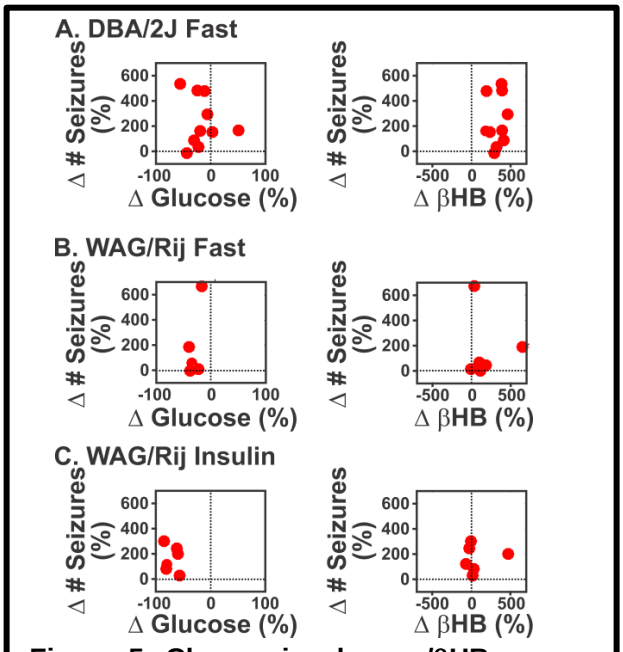

Figure 5. Change in glucose/βHB versus change in seizure count. A. *Left*: % change in glucose levels (before vs during fast) is plotted against % change in seizure count for each DBA/2J mouse. Points within the upper, left-hand quadrant identify animals with reduced blood glucose and increased seizure count during the fast. *Right*: % βHB change plotted against the % change in seizure count. **B, C.** Comparable analyses on the WAG/Rij fast and insulin experiments, respectively.

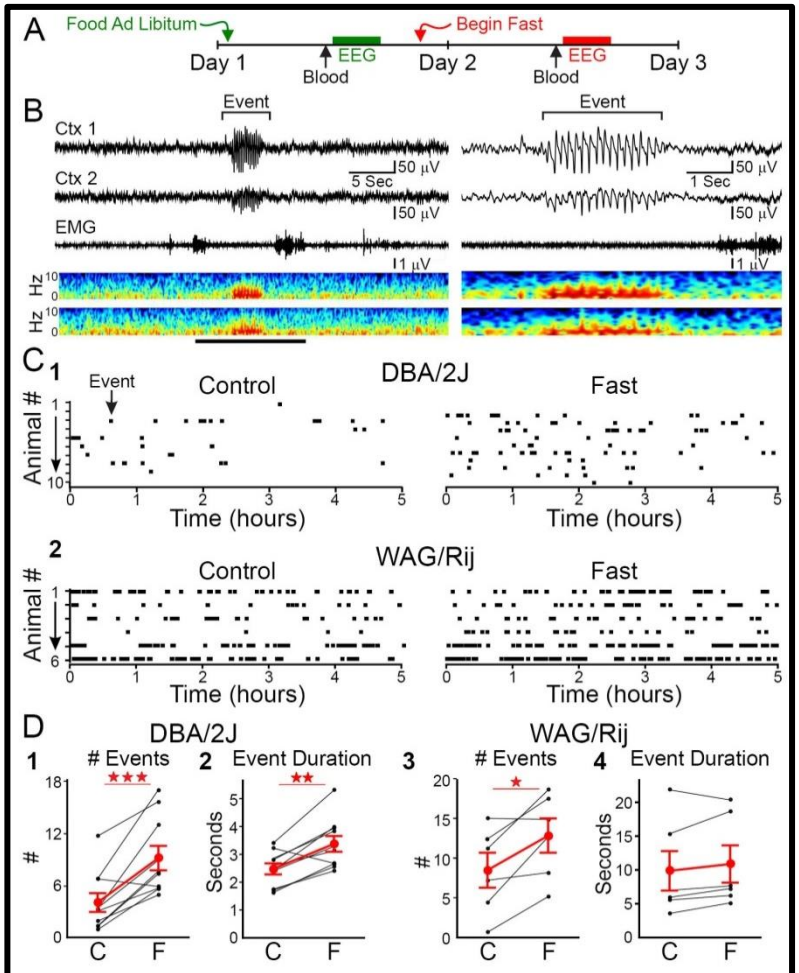

Figure 4. Elevated SWDs following fast. A. Experiment. **B.** SWD recorded in a DBA/2J mouse. Recordings on left are on compressed time scale. Recordings on right correspond to region defined by black bar on left. Two cortical (ctx) and one muscle (EMG) recording are shown. Spectrograms below recordings highlight elevated power in 3-7Hz range during the event. **C.** Seizures per DBA/2J (top) and WAG/Rij (bottom) presented in raster format before and during the fast. SWDs are represented by black squares. **D.** Analyses for all DBA/2J mice (1,2) and WAG/Rij rats (3,4) during control (C) and fast (F).

The dissociation of βHB levels from insulin-triggered absence seizures is notable. Some have argued that the observation of fasting-triggered SWDs conflicts with the rich literature establishing the efficacy of the ketogenic diet in the treatment of epilepsy[13]. If ketone bodies are elevated following an acute fast *and* during the ketogenic diet, then how could they promote seizures in the former condition while reduce seizures in the latter? However, this paradox only exists if one assumes that ketone bodies *are* responsible for seizure exacerbation during the acute fast. Our insulin data suggest that ketone bodies play little role, consistent with a recent finding showing that ketone bodies are not responsible for decreased nervous system excitability during the ketogenic diet[68]. In contrast, the persistent inverse correlation between glucose and SWDs observed across multiple manipulations supports the hypothesis that absence seizures are exacerbated by low glucose.

2.1.D. Thalamocortical circuit engagement is elevated during hypoglycemia.

A fundamental question arises from our preliminary EEG investigation into SWDs triggered by hypoglycemia: does the thalamus, a critical absence seizure-generating node, directly contribute to the increased occurrence of SWDs during periods of low blood glucose? One approach to evaluate thalamic involvement is to determine whether blood glucose levels alter functional connections among brain structures using resting state functional magnetic resonance imaging (R-fMRI).

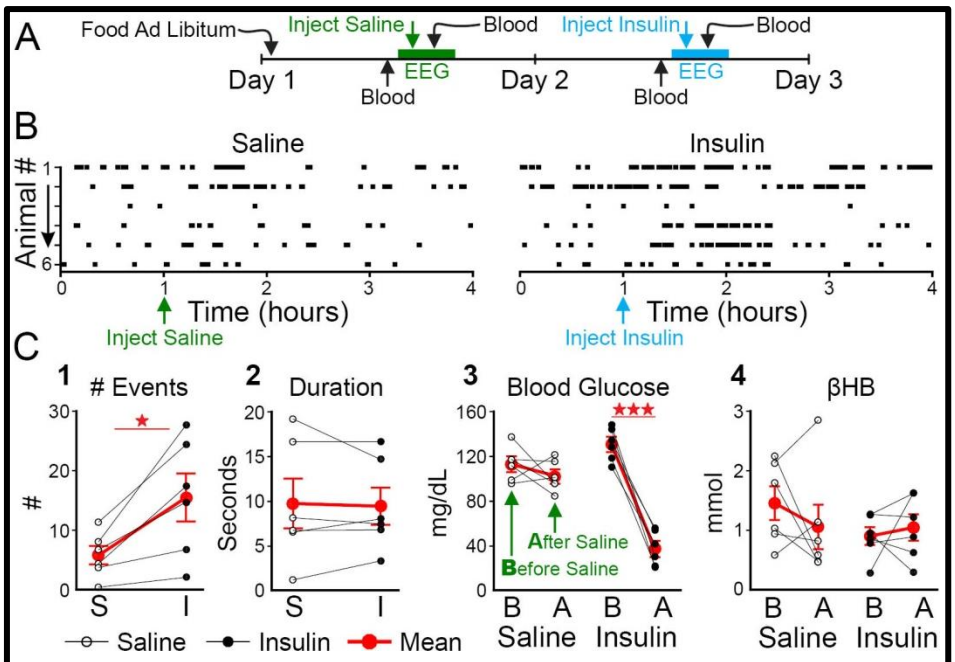

Figure 6. Insulin injection into WAG/Rij rats. A. Experiment. **B.** All seizures per WAG/Rij presented in raster format before and following saline (left) and insulin (3.0 IU/kg, right) injection. SWDs are represented by black squares. Injection occurred one hour after initiating the recording. **C.** Population. The number of SWD events **(1)** and event duration **(2)** is plotted for each animal's saline (S) and insulin (I) injection. Measurements of blood glucose **(3)** and βHB **(4)** before (B) and after (A) saline/insulin injection. Saline injections did not change levels of blood glucose or βHB. Insulin injections reduced blood glucose levels and did not affect βHB levels.

R-fMRI, an outgrowth of conventional fMRI, does not measure putative neural activation during a specific task[69-71]. Instead, R-fMRI measures the subject at rest, and assumes that certain regions of the brain will be active. By extension, regions that are functionally connected will be coactive and will co-vary in their fMRI-associated blood oxygenation level dependent (BOLD) signals. We assessed functional connectivity among brain regions in fed and fasted DBA/2J mice.

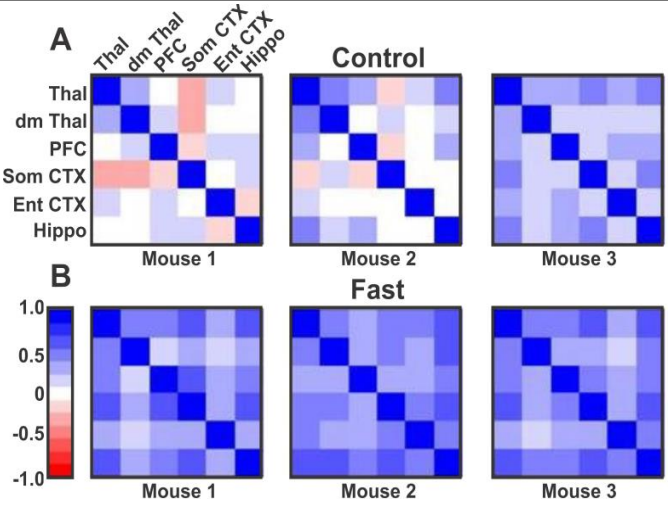

Figure 7. Resting state fMRI. A. Correlation matrices derived from resting state fMRI scans of three fed mice. Structures compared include thalamus (Thal), mediodorsal thalamus (mdThal), prefrontal cortex (PFC), somatosensory cortex (somCTX), entorhinal cortex (EntCTX) and hippocampus (Hippo). Dark blue represents strong and positive correlations (i.e. strong functional connections) between two structures. Red represents strong and negative correlations. **B.** Matrices from the same animals following a fast.

Similar to our EEG experiments, we performed R-fMRI experiments in mice on two consecutive days. R-fMRI was performed in a 7 Tesla small animal MRI maintained by the University of Virginia School of Medicine Molecular Imaging Core. Before the first scan, the animals ate *ad libitum*. After the first scan, food was removed and the animals were recorded again after a 16 hour fast. R-fMRI data was analyzed in collaboration with Dr. Nick Tustison, an expert consultant on this proposal and co-developer of Advanced Normalization Tools for R (ANTsR). ANTsR was developed by the University of Pennsylvania's *Penn Image Computing & Science Lab* with the purpose of applying statistical measures to complex, three-dimensional functional imaging techniques.

While preliminary, functional connectivity increases among thalamocortical regions following an acute fast. The matrices shown in **Figure 7** reveal the degree of functional connectivity among regions. Each square within the matrix represents a comparison between two brain structures defined by an X-Y intersectional point. The color of each square indicates the degree to which the BOLD signal between the two structures correlates, dark blue representing a strong, positive correlation and dark red representing a strong, negative correlation. We restricted our analyses to cortical and thalamic structures, and the hippocampus.

The data indicate that acute fasting increases the functional connectivity (increases positive correlations) among structures of the thalamocortical axis. These results will be expanded upon below (section 3.1.D).

2.2. Data in support of Aim 2 (Hypothesis: *ATP-dependent potassium channels confer thalamocortical neurons with glucose sensitivity*).

Reciprocal connectivity between reticular thalamic (RT) and thalamocortical (TC) neurons of the ventrobasal nucleus is hypothesized to sustain SWDs[19,20,72]. During discharges, RT and TC neurons produce low-threshold, calcium spikes (LTS) mediated by the activation of T-type calcium channels[72-76]. When the LTS reaches the voltage for sodium channel activation, it is crowned with a barrage of rapidly occurring (200-400Hz) action potentials comprising a *burst*. Importantly, if T-type channels are largely inactivated, as occurs during a steady-state depolarization, then thalamic neurons are less likely to produce LTS-mediated bursts but resort to generating action potentials at a relatively low and regular (i.e. tonic) rate, hence the designation, *tonic* versus *burst* firing mode. LTS-mediated thalamic bursts sustain recurrent SWDs in absence epilepsy. Indeed, ethosuximide, a T-type calcium channel blocker, is used to treat absence seizures[1].

A critical property of T-type calcium channels is their dependence upon voltage hyperpolarization for subsequent activation. T-type calcium channels only transition to the open-state once inactivation is removed (i.e. *deinactivation*) by hyperpolarization. Thus, thalamic neurons produce LTS bursts during relatively hyperpolarized resting states. While counterintuitive, this paradoxical phenomenon of robust bursting elicited by hyperpolarization has long been attributed to neurons of the thalamus[77-79].

2.2.A. Thalamocortical neurons are glucose sensitive.

We performed patch clamp electrophysiology in acute brain slices to gauge the responsiveness of thalamic neurons to changing levels of energy substrates. We first used previously described strategies to assess glucose sensitivity[50,52,80]. Briefly, patch clamped neurons were recorded in the current-clamp configuration to measure resting membrane potential. Additionally, current injections were applied to assess excitability. Low glucose appeared to hyperpolarize thalamic neurons, therefore promoting bursting (**Fig. 8**).

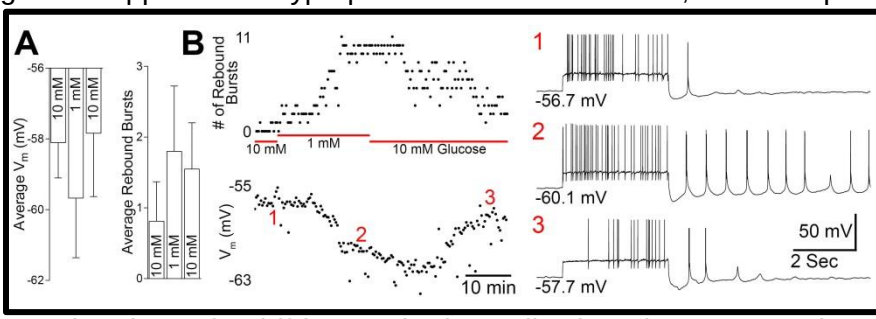

Figure 8. Glucose sensitivity of thalamic neurons. A. Whole-cell recordings from ventrobasal thalamic neurons. Exposure to low glucose (1 mM) trends toward hyperpolarization and an increase in rebound bursting elicited by brief depolarizing current injection (n=10). **B.** Representative response to low glucose, measured every 20 seconds (left) and raw trace (right).

We also determined if ketone body application alters neuronal excitability in the thalamus. Both in whole-cell (n>10) and cell-attached configuration (n=9), we were unable to elicit a consistent change in the excitability of either RT or TC neurons in response to βHB, even at high concentrations (>2mM, data not shown).

2.2.B. ATP-sensitive potassium channels localize to the thalamus.

Among ion channels, ATP-sensitive potassium (K_{ATP}) channels effectively transduce energy metabolism into neuronal activity[50,52,56,57]. Furthermore, glucose-mediated modulation of neuronal excitability in the ventromedial hypothalamus is mediated by K_{ATP} channels[50,52]. Collectively, these studies highlight the need to assess the role of these potassium channels in defining thalamic excitability. There is scant data addressing the thalamic expression of K_{ATP} channels and their role in defining thalamic excitability.

We used immunohistochemical approaches to stain for Kir6.2, the major subunit of the K_{ATP} channel. As an anatomical landmark, we stained for parvalbumin, a calcium binding protein prominently expressed in the RT nucleus. We observed widespread K_{ATP} channel expression throughout the brain, including the thalamus (**Fig. 9A1**). High magnification images resolved strong Kir6.2 expression in the dentate gyrus (**Fig. 9A2&C1**), consistent with previous reports[81,82]. Stain intensity was comparable in other regions (n=4).

We used molecular approaches to confirm K_{ATP} expression. *In situ* hybridization against mRNA transcribed from KCNj11, the gene encoding Kir6.2, indicated high levels of KCNj11 transcript in the dentate gyrus and comparable levels in both cortex and thalamus (**Fig. 9B**). Finally, we used qPCR to assess transcript levels and found similar KCNj11 copy number using a quantifiable standard (**Fig. 9C2, left**). We found comparable transcript levels using the house keeping gene cyclophilin-A as a reference (**Fig. 9C2, right**).

2.2.C. Thalamic K_{ATP} channel expression is functional.

Functional K_{ATP} channel expression was measured using electrophysiological techniques. Whole-cell patch clamp recordings of both RT and TC neurons in acute brain slices revealed strong, dose-dependent outward currents elicited by diazoxide, a K_{ATP} channel activator (**Fig. 9D1-2, 9E1-2**). These currents were blocked with

pre-application of glibenclamide, a K_{ATP} channel antagonist (**Fig. 9D3-4, 9E3-4**). Thus, in aggregate, our data demonstrate that neurons of the rodent thalamus express functional K_{ATP} channels.

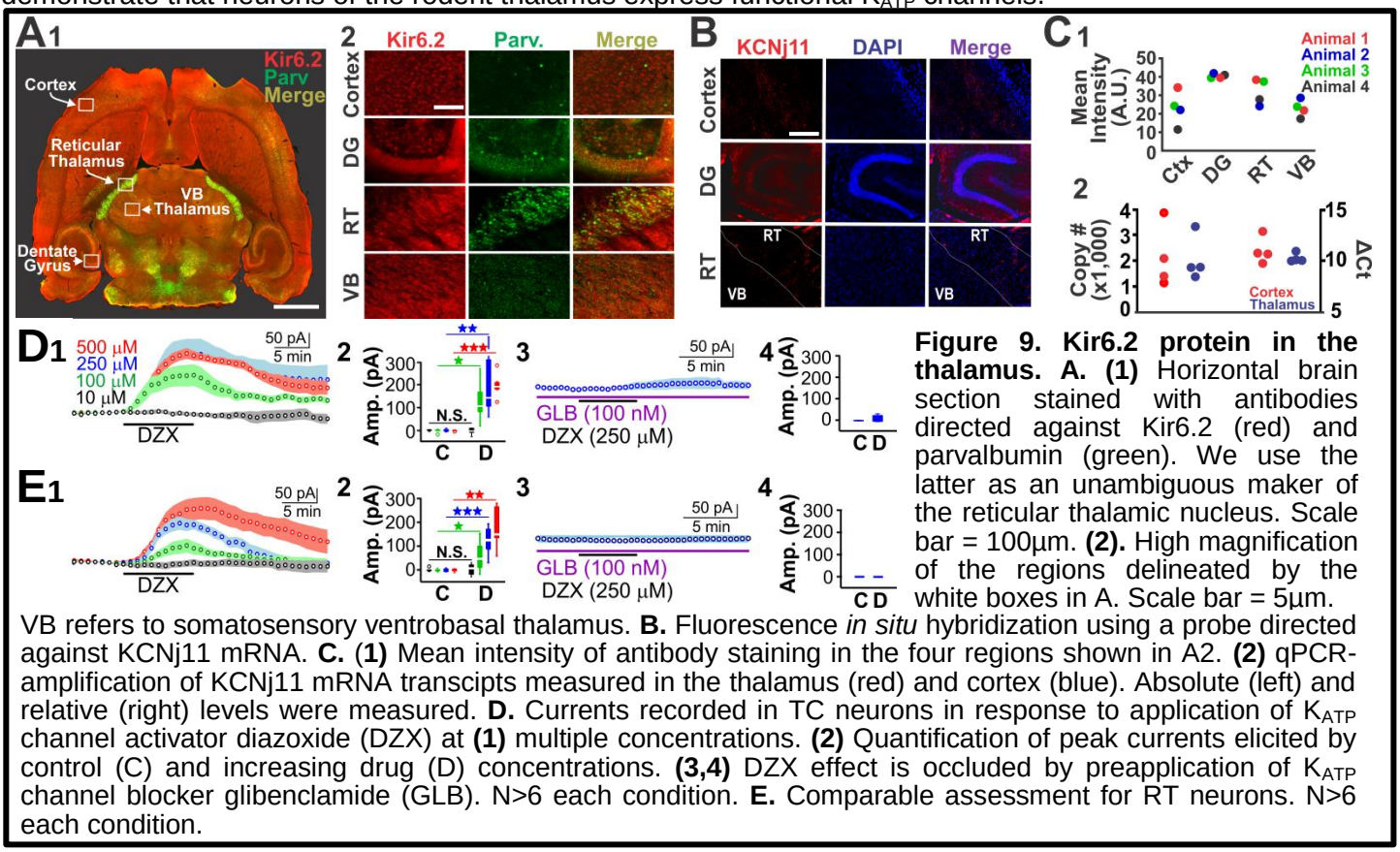

Figure 9. Kir6.2 protein in the thalamus. A. (1) Horizontal brain section stained with antibodies directed against Kir6.2 (red) and parvalbumin (green). We use the latter as an unambiguous maker of the reticular thalamic nucleus. Scale bar = 100μm. **(2).** High magnification of the regions delineated by the white boxes in A. Scale bar = 5μm. VB refers to somatosensory ventrobasal thalamus. **B.** Fluorescence *in situ* hybridization using a probe directed against KCNj11 mRNA. **C.** (**1**) Mean intensity of antibody staining in the four regions shown in A2. **(2)** qPCR-amplification of KCNj11 mRNA transcipts measured in the thalamus (red) and cortex (blue). Absolute (left) and relative (right) levels were measured. **D.** Currents recorded in TC neurons in response to application of K_{ATP} channel activator diazoxide (DZX) at **(1)** multiple concentrations. **(2)** Quantification of peak currents elicited by control (C) and increasing drug (D) concentrations. **(3,4)** DZX effect is occluded by preapplication of K_{ATP} channel blocker glibenclamide (GLB). N>6 each condition. **E.** Comparable assessment for RT neurons. N>6 each condition.

3. *Experimental Approach*

Our preliminary data support the overarching hypothesis that glucose directly modulates neural circuits in the thalamus to exacerbate seizures. We address this hypothesis with experiments outlined below performed on WAG/Rij rats. The first two Specific Aims are designed to define the mechanism(s) by which low blood glucose exacerbates absence seizures. The goal of the third Specific Aim is to determine how glucose modulates the responsiveness of absence seizures to anti-seizure drugs.

3.1 Specific Aim 1

Hypothesis: Low blood sugar is the primary trigger for elevated absence seizures during acute fasting.

Rationale: Our preliminary data support the hypothesis that hypoglycemia, not ketoacidosis, precipitates SWDs in two rodent models of absence seizures. We propose that increased SWDs result specifically from hypoglycemic conditions in the thalamus. Thus far, we have used blood glucose levels as a proxy for glucose levels in the brain. While brain-blood glucose levels are generally linearly related[83-85], we test the hypothesis that seizure exacerbation correlates with a reduction of glucose in the brain and, specifically, in the thalamus. We will use several approaches to measure brain and thalamic glucose levels.

Approach Glucose content in the brain will be measured in collaboration with Dr. Thurl Harris (consultant). Briefly, radiolabeled 2-deoxy-D-[1,2-^{3}H]-glucose (2-DG) will be injected into both fed and fasted animals. 2-DG is taken up by cells but does not undergo glycolysis. Brain, liver and white adipose fat will be harvested one hour after injection and both ^{3}H glucose (extracellular) and ^{3}H 2-deoxyglucose-5-phosphate glucose (intracellular) will be determined by scintillation counting.

Thalamic glucose will be measured with microdialysis techniques performed simultaneously with EEG recordings. In these experiments, WAG/Rij rats will be stereotaxically implanted with a microdialysis guide cannula into the ventrobasal thalamic nucleus and with EEG electrodes (see *General Methods*). Proof-of-principle experiments demonstrate our ability to target the ventrobasal nucleus for microdialysis while recording seizures. In these experiments (n=5), we delivered the $GABA_A$ receptor antagonist bicuculline methiodide (**BMI**) to the thalamus to elicit SWDs in naïve rats, as described before[86]. We observed multiple discharges within a few minutes of BMI infusion (**Fig. 10**). These results validate our successful use of this technique and support their use in the experiments proposed below.

3.1.A. ***Measure thalamic glucose with microdialysis*.** Microdialysis techniques are routinely used in awake and behaving rodents to measure chemicals[87], including glucose[85,88,89]. We will use this technique to directly

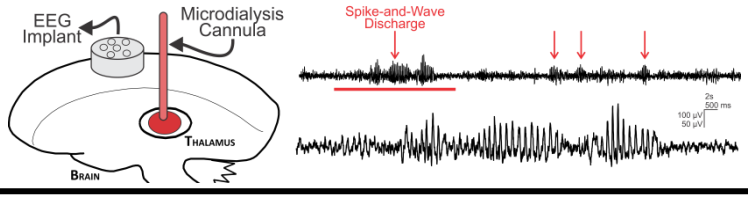

Figure 10. BMI microdialysis. EEG from naïve, Sprague Dawley rats infused with the $GABA_A$ receptor antagonist, BMI, through a microdialysis probe in the thalamic ventrobasal nucleus. We observed SWDs shortly after infusion, as previously described.

measure extracellular glucose in the thalamus while simultaneously recording EEG signals in WAG/Rij rats (see *General Methods*). We will record SWDs and continuously measure glucose before and during a fast (similar to **Fig. 3A**). Prior to each recording session, a calibrated microdialysis probe will be placed within the guide cannula. During the recording session, microdialysis effluent will be collected every 30 minutes and then measured for glucose using the no-net-flux[87,88,90] assay to obtain absolute concentration. Effluent ketone body levels will also be measured. Blood will be collected as before (**Fig. 3A**) to determine the degree of correlation between blood and microdialysis glucose levels. We will correlate energy substrate levels with SWD count.

Anticipated Results & Interpretation: As before, we anticipate that spike-and-wave occurrence will increase during the fasted period. We also expect that both blood, brain and microdialysis effluent will have lower glucose concentrations following the fast. If true, then we will conclude that spike-and-wave occurrence inversely correlates with thalamic glucose.

Pitfalls & Alternatives: Despite our proven success in performing microdialysis in rats, it remains possible that fasting-induced changes in thalamic glucose are too small to detect. If true, then we will perform comparable experiments with insulin injection, which produces a pronounced drop in glucose.

3.1.B. ***Selective inhibition of glucose metabolism in the thalamus*****.** The glucose analogue 5-thioglucose (5-TG)[85,91] is used to inhibit glycolysis by outcompeting endogenous glucose, producing a state known as *glucoprivation*. Injection of 5-TG into the ventromedial hypothalamus of behaving rats produces, within three hours, local glucoprivation and robust behavioral changes[85]. By extension, we will determine whether local thalamic glucoprivation is sufficient to precipitate SWDs in WAG/Rij rats. We will record from fed WAG/Rij rats implanted with both EEG electrodes and thalamic microdialysis guide cannulae.

As described by Dunn-Meynell et al.[85], we will compare the effects of two bolus deliveries through the guide cannula: 1µl saline with and without 5-TG (120µg). Before and after the saline injection, three hours of baseline EEG will be recorded. Then 5-TG will be injected and EEG will be recorded for an additional 4 hours, a time sufficient to observe any changes[85]. In a subset of animals, injection order will be reversed to ensure that seizure occurrence is not the result of repeated injections. SWD count from each of the three epochs (baseline, saline, 5-TG) will be compared. In a subset of animals, we will mix the 5-TG solution with rhodamine dextran beads to permit the visualization of solution spread within the thalamus. Animals will be sacrificed shortly after the recording session and beads will be localized.

Anticipated Results & Interpretation: Data from several studies indicate that neuronal activity of the thalamus is particularly vulnerable to low glucose levels[16-18,33]. Thus, we expect that local 5-TG delivery into the thalamus will increase the occurrence of SWDs. If true, then we will conclude that thalamic glucoprivation is sufficient to precipitate SWDs.

Pitfalls & Alternatives Unilateral thalamic injection of 5-TG may be insufficient to trigger seizures. If we find little effect on SWDs, these experiments will be replicated in animals implanted with bilateral cannula guides, one for each thalamus. Prolonged 5-TG delivery through a microdialysis probe, rather than bolus injections, may also allow for 5-TG to better spread throughout the thalamus. If neither uni- nor bi-lateral injections precipitate seizures, then we will directly inject βHB into the thalamus and quantify SWD occurrence, thereby testing the alternate hypothesis that other energy substrates modulate absence seizures.

3.1.C. ***Thalamic activity measurements during fasting*****.** We aim to directly measure thalamic activity during the progression from fed to fast, or from fed to insulin, in WAG/Rij rats. Several approaches can be used to measure neuronal activity *in vivo*. At present, we do not plan to use electrophysiological tools to record the activity of individual neurons, or small populations, within the thalamus; we are concerned that such techniques may be susceptible to incomplete sampling bias. Instead, we aim to record overall neuronal activity produced by the thalamus by measuring bulk fluorescence of thalamic neurons transfected with GCaMP6f, a genetically-encoded calcium indicator. We have implemented an approach recently developed by Dr. Karl Deisseroth's laboratory called fiber photometry[46] which permits the detection of small calcium indicator changes in deep subcortical structures. We are utilizing this approach to measure neuronal calcium changes in the thalamus.

GCaMP6 is delivered into the rodent brain using either intracerebroventricular or targeted stereotaxic injection (*General Methods*). Examination of acute brain slices from transfected rats reveals robust fluorescence changes in response to activity changes (n>5, **Fig. 11A&B**), thereby demonstrating that GCaMP6 is a good

proxy for neuronal activity in the thalamus. We can also record bulk GCaMP6 fluorescence *in vivo* in the thalamus of transfected WAG/Rij rats while monitoring their seizures (fiber photometry/EEG, **Fig. 11C**). Thus, in this sub-aim, we will simultaneously measure EEG signals and thalamic calcium activity in WAG/Rij rats before and during hypoglycemia. We will also quantify SWD occurrence.

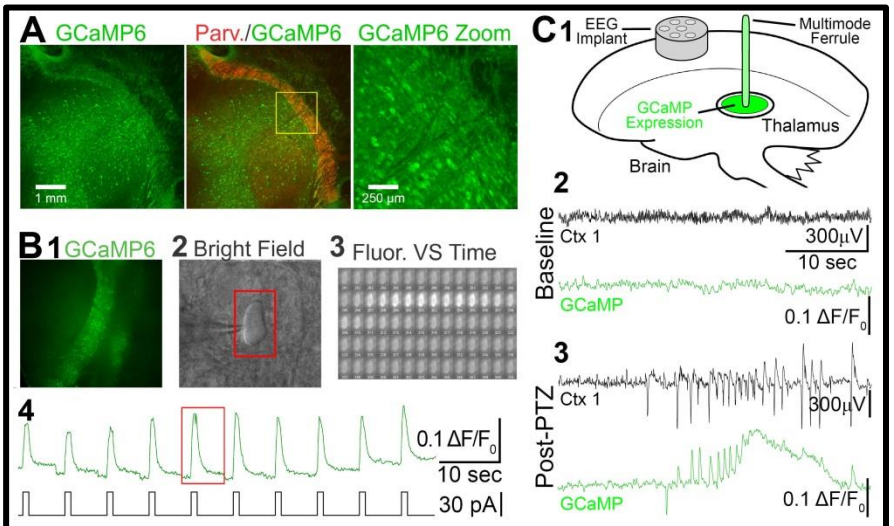

Figure 11. GCaMP signaling in the thalamus. A. Brain section from a P38 rat, 3 weeks after stereotaxic injection of AAV1-Syn-GCaMP6. Antibody staining against GFP (green, labels GCaMP) and parvalbumin (red) indicates GCaMP expression in both ventrobasal thalamic and reticular thalamic (RT) neurons. **B.** ICV injection of AAV1-Syn-GCaMP6 at P1 produced thalamic GCaMP expression by P16 **(1)**. Through whole-cell recording from an RT neuron **(2)** fluorescent responses were evoked (**3**, change in fluorescence over time, read left to right, top to bottom). GCaMP responses evoked by periodic current injections **(4)**. **C.** Fiber photometry allows *in vivo* recording of regional changes in GCaMP signal that can be correlated with EEG **(1)**. Baseline thalamic activation was low **(2)**, but increased in concordance with pentylenetetrazol injection (PTZ) **(3)**.

Anticipated Results & Interpretation: Human studies demonstrate that hypoglycemia elevates putative neuronal activity in the thalamus[92,93]. We hypothesize that the same occurs in rats. Thus, we anticipate that population calcium signals measured in the thalamus will be elevated, relative to control conditions, following an overnight fast and following an insulin injection. If true, then we will conclude that hypoglycemia elevates neuronal activity in the rat thalamus.

Pitfalls & Alternatives: Our experiments specifically address hypoglycemia-associated changes in thalamic activity. However, the activity of other, absence seizure-associated brain structures may be similarly glucose sensitive. To address this possibility, we will implant an optical fiber within the peri-oral region of somatosensory cortex of WAG/Rij rats and measure activity before and during hypoglycemia. Relative fluorescence changes will be compared with those measured from the thalamus to determine whether the rat thalamus, like its human counterpart, is selectively glucose sensitive. Finally, while fiber photometry is highly sensitive, it remains possible that only a subset of thalamic neurons responds to hypoglycemic conditions, and that the fluorescence changes associated with those neurons are undetectable using the bulk imaging approach. However, this is unlikely as human PET scans suggest that robust changes in thalamic activity occur during hypoglycemia. Nonetheless, if we find no fluorescence change in response to hypoglycemia, then we will utilize conventional electrophysiological approaches to record neuronal activity in the thalamus (e.g. depth electrode). Our expert consultant, Dr. Jaideep Kapur, has extensive experience with combining rodent EEG with subcortical depth electrode recordings.

3.1.D. *Hypoglycemia increases functional thalamocortical connectivity*.

Approach. We will follow the same procedures outlined in section 2.1.D to assess hypoglycemia-induced changes in WAG/Rij functional brain connectivity. In brief, we will run R-fMRI scans on two consecutive days. After the first day (i.e. control), animals will be fasted immediately following their scan so that they will be ready for the next day's scan (i.e. fast). We will also induce hypoglycemia with insulin. Accordingly, animals will be injected with saline prior to the scan on day one, and with insulin prior to the scan on day two. Functional connectivity will be assessed with Ants-R in collaboration with Dr. Nick Tustison (see section 2.1.D).

Anticipated Results & Interpretation: We expect to replicate our preliminary data indicating that hypoglycemia enhances functional connectivity along the thalamocortical axis.

Pitfalls & Alternatives: Animals may seize during the scan. If true, then it is formally possible that SWDs produced during the scan bias the correlation matrices towards strong functional connectivity among cortical and thalamic regions. While perhaps interesting, such a correlation would not be particularly surprising, nor would one expect to find a significant difference among fed and fasted rats as both cohorts produce seizures (although one cohort produces more than the other). More interesting is the functional connectivity during the *non-seizure* state. If fasted rats are more disposed to seize, and if they do so because the thalamus is hyperexcitable during conditions of low blood glucose, then one would expect to find greater functional connectivity throughout the basal state. To address the possibility of seizure-bias in our connectivity assessment, we will perform simultaneous EEG and R-fMRI recordings and compare values derived from the

full scan to portions of the scan that do not include seizures. John Williamson, long-time and highly-skilled EEG specialist with Dr. Jaideep Kapur, has experience performing these recordings.

3.2 Specific Aim 2

Hypothesis: ATP-dependent potassium channels confer thalamocortical neurons with glucose sensitivity.

Rationale: Thus far, we have established that thalamic neurons are glucose sensitive, and that thalamic neurons respond to low glucose by bursting. These observations are consistent with the hypothesis that thalamic neurons hyperpolarize during periods of low glucose. While a potassium conductance such as one produced by open K_{ATP} channels could account for such hyperpolarization, we have yet to demonstrate this possibility. In this aim we will first establish the bounds of glucose sensitivity by performing dose-response experiments. We will then test the hypothesis that K_{ATP} channels mediate thalamic glucose sensitivity.

Approach: We will utilize our lab's expertise to perform acute brain slice experiments (*General Methods*) designed to assess both cellular and circuit-level excitability.

3.2.A. ***Establish parameters of glucosensitivity associated with thalamic neurons.*** Our patch clamp data demonstrate that acute hypoglycemia elicits bursting behavior of thalamocortical (TC) neurons of the ventrobasal nucleus (**Fig. 8**). These changes were elicited by a large drop in glucose concentration (10mM to 1mM). In these experiments we will fully characterize glucose responsivity across a full range of concentrations (0, 1, 2, 5, 10mM). Comparable experiments have been performed in the ventromedial hypothalamus[50,52]. As in our preliminary data, we will first measure membrane potential and bursting behavior electrophysiologically in the current-clamp configuration. In one set of experiments, we perfuse brain slices with 10mM glucose concentration (control) and then systematically lower the bath glucose concentration to either 5, 2, 1, or 0 mM glucose. To ensure proper wash and reversibility, the response elicited by each cell will be challenged by only a single glucose concentration. In a second set of experiments, 5mM glucose concentration will serve as our control condition.

In a parallel set of studies, we will determine dose-response relationships of neurons recorded in the voltage-clamp configuration. Neurons will be clamped at -50mV so that conductance changes in any of the major ionic species, including potassium, can be observed (-50mV is sufficiently different from the equilibrium potentials for calcium, sodium, chloride and potassium). As before, neurons will be recorded in the control condition for 10 minutes and then for 15 minutes in altered glucose, followed by a wash.

Anticipated Results & Interpretation: Our preliminary data are consistent with the hypothesis that a hyperpolarizing conductance is activated during hypoglycemia. As there is precedence for K_{ATP} channel activation during episodes of low glucose[50,52], we anticipate that thalamic neurons will respond with (1) a hyperpolarization in the current-clamp configuration, and (2) an outward current when voltage-clamped. We anticipate that these effects will be dose-dependent. Finally, we also expect to observe greater bursting behavior in low glucose perfusates. If true, then we will conclude that thalamic neurons are glucose sensitive and display an increased propensity to burst in low glucose.

Pitfalls & Alternatives: Initially, we will focus our recording efforts on thalamocortical neurons of the ventrobasal nucleus. However, if these neurons display only modest glucose sensitivity, we will extend our glucose characterization to the reticular thalamic nucleus. Our data demonstrate that these neurons also express K_{ATP} channels (**Fig. 9**). In the unlikely possibility that neither neuronal population responds to glucose, we will shift our attention to the possibility that βHB directly modulates neurons of the thalamus.

3.2.B. ***Identify molecular basis of glucosensitivity.*** We will begin by determining whether channels open or close in response to low glucose. First, we will voltage-clamp neurons and periodically (once per 15 sec) deliver brief (200ms), small (Δ5mV) hyperpolarizing voltage excursions from the -50mV holding voltage throughout the control and altered glucose recording. By so doing, we will be able to determine whether glucose elicits an increase in membrane resistance, indicative of channel closure, or a decrease in membrane resistance, indicative of channel opening. In the same cells and interleaved with the periodic voltage steps, we will also deliver a slow voltage ramp ranging from -120mV to -80mV. We will fit the current response to the voltage ramp with a straight line to estimate the whole-cell conductance before and during low glucose. The latter protocol has been used to assess K_{ATP}-mediated changes in conductance. To disambiguate potassium from chloride conductances, we will perform a subset of voltage-clamp experiments with pipette solutions containing an elevated concentration of chloride. By doing so, any glucose-mediated activation of a chloride conductance will be associated with an inward, or depolarizing, shift.

The aforementioned experiments provide significant insight into the ionic basis of glucose-mediated changes. However, the experiments are unlikely to resolve the specific channel subtype involved. To that end, we will use pharmacological manipulations to parse out the role of K_{ATP} channels using the many relatively selective

activity modulators for this channel. Glucose responsivity in voltage-clamped neurons will be assessed by changing glucose levels in slices *preincubated* with either glibenclamide, a K_{ATP} channel blocker, or diazoxide, a K_{ATP} channel opener (**Fig. 9**).

Anticipated Results & Interpretation: We anticipate that low glucose-mediated hyperpolarization will result from potassium channel opening. Because decreased membrane resistance is associated with channel opening, we expect that larger current injections will be required to maintain the small, Δ5mV hyperpolarizing steps (V=IR; if R decreases, I must increase to maintain V). Consistent with this observation, we expect that whole-cell membrane conductance (g=1/R) will increase during low glucose. We also expect that this conductance will be associated with a relatively hyperpolarized reversal potential (~-90mV), indicative of potassium acting as a charge carrier. Finally, we anticipate that glucose-mediated changes in the electrical properties of thalamic cells will be blocked by glibenclamide (channel block) and preempted by diazoxide (occlusion block). The latter should occur because K_{ATP} channels opened by diazoxide would be unavailable for opening by low glucose. If we observe these collective responses, then we will conclude that K_{ATP} channels confer glucose sensitivity to thalamic neurons.

Pitfalls & Alternatives: If K_{ATP} channels do not mediate the observed glucose sensitivity, then we will perform additional pharmacological experiments. Glucose is known to modulate the whole-cell conductance of hippocampal neurons by activating G protein-coupled adenosine receptors (A_1R) that, in turn, activate K^+-conductances. If true, then glucose-mediated changes would be blocked by the A_1R antagonist DPCPX[80].

3.2.C. ***Determine glucose sensitivity of in vitro epileptiform oscillations.*** Here we assess glucose sensitivity of network oscillations. The acute thalamic slice preparation has served as a useful tool to understand thalamic circuit dynamics underlying both normal and epileptiform oscillations[94-100]. Under normal conditions, relatively fast, non-pathological network oscillations (~10Hz) persisting for 5-10 seconds can be reliably evoked by delivering an electrical stimulus to corticothalamic fibers innervating the slice. These oscillations can be pharmacologically transformed, for example with BMI, into oscillations that resemble SWDs. Using this approach, we will evoke *in vitro*, thalamic network oscillations (one per 60 seconds) in control solution (10mM glucose), and then in solution containing low glucose (0-5mM). Evoked oscillation parameters such as duration, frequency and oscillatory index[100] will be measured.

Anticipated Results & Interpretation: Low glucose promotes bursting behavior of individual thalamocortical neurons. Therefore, we anticipate that normal oscillations will become prolonged, slower and hypersynchronous in low glucose. If true, then we will conclude that *in vitro* thalamic oscillations become more epileptiform in low glucose.

Pitfalls & Alternatives: If normal oscillations are not transformed by low glucose, then we will examine the effects of glucose concentration manipulations on epileptiform (e.g. BMI-induced) oscillations[99,100].

3.3 Specific Aim 3

Hypothesis: Diet modulates the effectiveness of anti-absence seizure drugs.

Rationale: Anti-absence seizure drug ethosuximide dampens the excitability of thalamic neurons by blocking T-type calcium channels. Ethosuximide completely abolishes SWDs in WAG/Rij rats (**Fig. 12**). Our data suggest that hypoglycemia promotes T-type channel-mediated bursting in thalamic neurons. The opposing actions of ethosuximide and hypoglycemia likely compete to determine thalamic neuron excitability.

Approach: We will determine the dose-response actions of ethosuximide in fed and fasted WAG/Rij rats. 4 doses will be delivered in random order to each animal: 0, 50, 100, and 150 mg/kg[101]. One intraperitoneally-delivered dose will be used on each animal per day, and dose evaluations will occur every other day to ensure complete drug clearance. Each dose will be tested in both the fed and fasted conditions. Blood glucose will be measured prior to each EEG recording. Fasted animals will only be assessed if their blood glucose levels drop by 25-35%. Each recording will consist of a three hour baseline period, followed by the saline/drug injection and then an additional three hours of recording. SWD count will serve as our response parameter.

Anticipated Results & Interpretation: We anticipate that the dose-response curve for fasted animals will be rightward-shifted relative to the fed animals, indicating that a higher ethosuximide dose is required in the fasted condition to achieve the comparable SWD reduction observed in the fed condition.

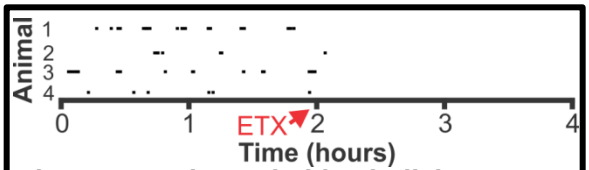

Figure 12. Ethosuximide abolishes SWDs in WAG/Rij. Raster of SWD activity before and after intraperitoneal injection of 200mg/kg ethosuximide (ETX, n=4).

Pitfalls & Alternatives: Ethosuximide dose and SWD count may have a very steep relationship, making it difficult to discern differences between the fed and fasted conditions. If true, then we will use duration of SWD cessation as our response parameter (i.e. latency to first SWD using as our start point 5 minutes post-injection). Finally, if a complete

dose-response curve proves challenging to acquire, then we will use only two ethosuximide doses (50 and 100mg/kg), as has been reported for the additive effects of glutamate receptor blockers and ethosuximide on SWD count[101]. Each of the two doses will be evaluated in the fed and fasted animals. Finally, effects of diet on the dose-response actions of other anti-absence seizure drugs will be tested.

	Experiment	Parameter	$Mean_{Control}$ ± SEM	$Mean_{Manipulation}$ ± SEM	p-Value	Sample Size	Power	Target N (with power = 0.8)
DBA/2J	Fast	# of Seizures	4.11 ± 1.1	9.35 ± 1.43	$8.2x10^{-4}$	10	0.99	6
		Seizure Duration	2.47 ± 0.19	3.37 ± 0.28	0.002	10	0.98	6
		Seizure Burden	2.4 ± 0.8	6.2 ±1.1	0.009	10	0.99	8
		Glucose	169.7 ± 12.9	138.6 ± 10.9	0.029	12	0.57	19
		Ketone Bodies	2.0 ± 0.2	7.4 ± 0.9	$5.9x10^{-5}$	12	1.0	3
WAG/Rij	Fast	# of Seizures	8.47 ± 2.2	12.8 ± 2.2	0.025	6	0.36	15
		Seizure Duration	9.86 ± 2.9	10.6 ± 2.8	0.18	6	0.06	405
		Seizure Burden	137.8 ± 64.1	252.0 ± 106.1	0.049	6	0.31	27
		Glucose	112.8 ± 5.7	80.6 ± 4.6	$1.6x10^{-4}$	11	0.99	5
		Ketone Bodies	1.03 ± 0.11	4.8 ± 0.7	0.0011	6	1	3
WAG/Rij	Insulin	# of Seizures	5.72 ± 1.6	13.7 ± 3.7	0.043	6	0.98	6
		Seizure Duration	9.7 ± 2.8	13.7 ± 13.7	0.77	6	0.051	6,998
		Seizure Burden	47.8 ± 20.3	94.2 ± 38.1	0.12	6	0.46	17
		Glucose	131.3 ± 6.21	37.33 ± 6.0	$1.98x10^{-4}$	6	1	3
		Ketone Bodies	0.91 ± 0.15	1.05 ± 0.22	0.62	6	0.13	83

Table 1. Statistical power analyses for preliminary EEG & blood data.

4. General Methods

Slice Preparation – Acute brain slices will be prepared from P20-40 animals using the protective recovery method[102]. Briefly, anesthetized animals will be transcardially perfused with ice-cold NMDG aCSF, containing (in mM): 92 NMDG, 2.5 KCl, 1.25 NaH_2PO_4, 26 $NaHCO_3$, 20 HEPES, 25 glucose, 2 thiourea, 5 Na-ascorbate, 3 Na-pyruvate, 0.5 $CaCl_2$, 10 $MgSO_4$, pH of 7.4. All solutions will be bubbled with 95% O_2/5% CO_2. 250µm thick horizontal slices containing the thalamus will be collected using a vibrotome (Leica Microsystems) and incubated (34°C) for 15 minutes in NMDG aCSF. Slices will then be transferred to 21°C, recording aCSF, containing (in mM): 126 NaCl, 2.5 KCl, 1.25 NaH_2PO_4, 26 $NaHCO_3$, 10 glucose, 2 $CaCl_2$, 1 $MgSO_4$.

Intracellular Recordings – Glass recording pipettes will be pulled with a P-1000 puller (Sutter Instruments). Potassium gluconate pipette solution will be used, containing (in mM): 100 K-gluconate, 13 KCl, 10 EGTA, 10 HEPES, 9 $MgCl_2$, 0.07 $CaCl_2$, 2 Na_2-ATP, 0.5 Na-GTP, pH of 7.4, 280-285 mOsm/l. Voltage- and current-clamp recordings will be acquired with a Multiclamp 700B amplifier using pClamp software (Axon Instruments).

EEG Recordings – Animals will be anesthetized with isoflurane and secured in a stereotaxic frame. The exposed cranium will be cleaned and 0.6mm holes will be drilled through the skull for cortical electrodes above each hemisphere and a cerebellar reference. Steel screw electrodes will be inserted into each hole. Then, an EMG electrode will be sutured to the neck muscle. Electrodes are secured using dental cement. See *Vertebrate Animal* section for post-operative care. EEG recordings will be acquired with a differential amplifier (A-M Systems) and digitizer (AD Instruments). Wireless EEG is recorded with Epoch devices (Epitel) and similarly digitized. Synchronized video is recorded simultaneously for all EEG experiments. A subset of EEG experiments will also be performed in combination with:

Microdialysis – Microdialysis guide cannula will be stereotaxically implanted into the thalamic ventrobasal nucleus. Dialysis will be performed by delivering solution, through a microdialysis probe inserted into the cannula, with a syringe pump (Harvard Apparatus). Effluent solution will be collected for analysis.

Fiber Photometry – Multimode ferrule will be stereotaxically implanted into the thalamic ventrobasal nucleus. GCaMP (see below) will be excited using a patch cord delivering 473nm light from a diode laser (Omicron Luxx) and emission will be recorded using a photoreceiver (Newport)[46].

GCaMP Delivery – GCaMP6 indicator expression will be achieved by either intracerebroventricular (ICV) or stereotaxic injection of an AAV viral vector (Penn Vector Core). ICV delivery will be performed by injecting vector into the lateral ventricle of P0-2 animals. Stereotaxic delivery will be performed by pressure ejection of vector directly into the thalamus of adolescent animals. See details in *Vertebrate Animal* section.

***In Vitro* Calcium Imaging –** Brain slices will be prepared as above. Activity-associated changes in GCaMP signals will be recorded using an sCMOS camera (Hamamatsu).